Check for updates

Journal of
Materials Chemistry C
Materials for optical, magnetic and electronic devices

Accepted Manuscript

This article can be cited before page numbers have been issued, to do this please use: M. Perego, F. Caruso, G. Seguini, E. Arduca, R. Mantovan, K. Sparnacci and M. Laus, *J. Mater. Chem. C*, 2020, DOI: 10.1039/D0TC01856B.

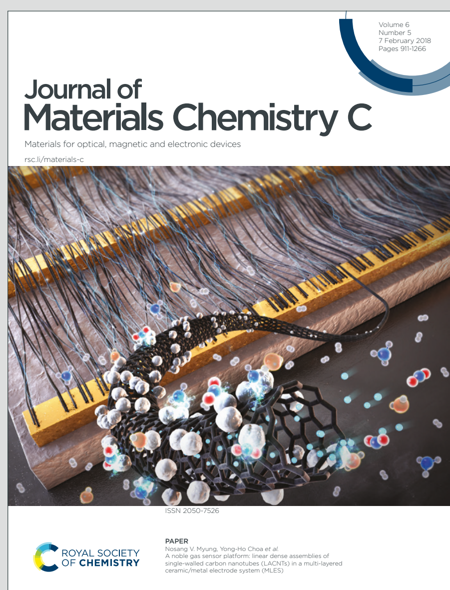

This is an Accepted Manuscript, which has been through the Royal Society of Chemistry peer review process and has been accepted for publication.

Accepted Manuscripts are published online shortly after acceptance, before technical editing, formatting and proof reading. Using this free service, authors can make their results available to the community, in citable form, before we publish the edited article. We will replace this Accepted Manuscript with the edited and formatted Advance Article as soon as it is available.

You can find more information about Accepted Manuscripts in the Information for Authors.

Please note that technical editing may introduce minor changes to the text and/or graphics, which may alter content. The journal's standard Terms & Conditions and the Ethical guidelines still apply. In no event shall the Royal Society of Chemistry be held responsible for any errors or omissions in this Accepted Manuscript or any consequences arising from the use of any information it contains.

ROYAL SOCIETY OF CHEMISTRY

rsc.li/materials-c

View Article Online
DOI: 10.1039/D0TC01856B

ARTICLE

Doping of Silicon by Phosphorus End-Terminated Polymers: Drive-in and Activation of Dopants

Received 00th January 20xx,
Accepted 00th January 20xx

DOI: 10.1039/x0xx00000x

Michele Perego,*[a] Francesco Caruso[a,b], Gabriele Seguini[a], Elisa Arduca[a], Roberto Mantovan[a], Katia Sparnacci[c] and Michele Laus.[c]

An effective doping technology for precise control of P atom injection and activation into a semiconductor substrate is presented. Polystyrene polymers with narrow molecular weight distribution and end-terminated with a P containing moiety are used to build up a phosphorus δ-layer to be employed as dopant source. P-atoms are efficiently injected into the Si substrate by high temperature (900-1250°C) thermal treatments. Temperature dependent (100-300 K) resistivity and Hall measurements in the Van der Pauw configuration, demonstrate high activation rates (η_a > 80%) of injected P atoms. This bottom-up approach holds promises for the development of a mild technology for efficient doping of semiconductors.

Introduction

Semiconductor technology relies on the capability to tune the electrical properties of the substrate through the controlled introduction of substitutional impurities (doping) in the crystal lattice of the semiconductor host material, in order to tailor its electronic, optical and/or magnetic properties.[1] However, present *ex situ* doping strategies cannot be easily extended to the nanoscale. As the size of semiconductor devices shrinks to the nanoscale, the standard random distribution of the individual atoms within the semiconductor becomes critical since the assumption of uniform doping distribution does not hold anymore.[2-3] Currently there is a significant effort of the scientific community for the development of a new technology to demonstrate deterministic doping of semiconductor structures at nanoscale.

Conventional doping techniques are mainly based on ion implantation which implies the bombardment of the target semiconductor with high energy dopant-containing ions that, subsequently, are induced to replace atoms in the lattice using a high temperature thermal treatment.[1] The main advantage of this technique is the independent control of the dopant dose and depth distribution of the impurity atoms within the semiconductor host. This approach has been widely explored, becoming the workhorse in microelectronics, since it guarantees excellent doping uniformity over large areas. Nevertheless, there is a number of drawbacks that are associated with ion implantation technology, including damage of the crystal lattice during ion bombardment and subsequent transient enhanced diffusion caused by defects during the thermal treatment.[4] Moreover, most of the source gases, commonly used in ion implantation, are hazardous from health and environmental perspective.[5] Finally, this technique is incompatible with 3D nanostructured materials since it does not provide conformal dopant incorporation for non-planar nanostructures.[6]

Plasma immersion ion implantation, also referred as plasma doping, is an emerging technique based on the extraction of accelerated ions from a plasma by applying high voltage in order to implant them in a semiconductor substrate.[7] This technique offers significant advantages over conventional ion implantation, since the doping profiles are generally more conformal than those obtained using conventional ion implantation. However, even in this case, there are several problems due to crystal damages and, at the same time, difficulties in doping with multiple species at different energies in a single process.[5] Moreover, all these ion-based approaches present significant drawbacks when applied to compound semiconductors composed by two or more chemically and electronically non-equivalent lattice sites, since the stoichiometry of the target matrix can be locally modified from implantation induced crystal damage.[1]

Alternative approaches based on gas phase or solid phase diffusion have been investigated as well, but they face fundamental limits in controlling dopant concentration near the surface and lack of uniformity.[1] Spin-on doping technology consists of depositing a dopant-containing solution onto the semiconductor surface, followed by a diffusion-annealing step. The dopant-containing solution is usually formed by either a mixture of SiO_2 and dopant atoms or Si-containing polymers with dopant atoms incorporated into the polymeric chains, like phosphosilicates or borosilicates.[8] Unfortunately, this simple and nondestructive technique does not guarantee accurate dose control over large areas of the substrate. In addition, residues left over from the solution containing the dopant

a. CNR-IMM Agrate Unit, Via C. Olivetti 2, I-20864 Agrate Brianza, Italy
b. Università degli Studi di Milano, Via Celoria 16, I-20133 Milano, Italy
c. Università del Piemonte Orientale ''A. Avogadro'', Viale T. Michel 11, I-15121 Alessandria, Italy

Electronic Supplementary Information (ESI) available: [details of any supplementary information available should be included here]. See DOI: 10.1039/x0xx00000x

Published on 19 May 2020. Downloaded by Uppsala University on 5/20/2020 3:40:09 PM.

Journal of Materials Chemistry C Accepted Manuscript

View Article Online
DOI: 10.1039/D0TC01856G

Published on 19 May 2020. Downloaded by Uppsala University on 5/20/2020 3:40:09 PM.

precursor are not easily removed from the surface, resulting in a chemically modified layer very difficult to be stripped off.[5] Self-assembling strategies followed by molecule grafting have been demonstrated to be effective in generating a uniform monolayer of dopant-containing molecules tethered to the pristine crystalline Si substrates over large areas.[9] Assuming a sufficiently high number of reactive sites on the substrates, the effective density of grafted molecules is ultimately determined by the molecule footprint. This self-limiting reaction has been used in combination with conventional spike annealing to enable the formation of B, P and As sub-5 nm ultra-shallow junctions in Si.[6,9-11] Nanoscale doping of InAs,[12,13] $In_xGA_yAs_z$,[14,15] InP[16], Ge[17-19] and SiGe[20] via monolayers of dopant containing molecules has been demonstrated as well. This gentle approach, usually referred as monolayer doping (MLD), has been proven to be efficient in introducing controlled amounts of dopants in Si nanowires[9] and InP nanopillars.[16] MLD is very versatile as, in principle, surface preparation, molecular footprint, capping layer and thermal treatment parameters can be finely tuned to optimize surface coverage of the molecules and diffusion of the dopant into the semiconductor. However, the wet chemistry commonly used in the MLD process significantly limits the manufacturability of this process technology.[9] Moreover, dopant concentrations obtained by MLD are ~ 10^{20} cm^{-3}. The extension of this approach to doping concentrations in the range 10^{15}-10^{21} cm^{-3} is essential for its industrial exploitation. A modified MLD approach was proposed as a strategy to reproducibly control the doping dose.[21] The dopant-containing molecules are mixed with dopant free molecules and subsequently grafted onto the Si surface. The final monolayer composition is assumed to be proportional to the fraction of dopant-containing molecules in the solution. In this way, the doping dose was varied over 1 order of magnitude, but reproducibility and accuracy of this approach are questionable.[21] Finally carbon and oxygen contamination can be introduced in the silicon substrate during the drive-in process, forming complex defects that affect the electrical properties of the semiconductor substrate. Interstitial carbon can form pairs with group-V dopants, like phosphorus, arsenic and antimony, creating multiple deep energy levels into the gap of the semiconductor.[22] Carbon related defects have been reported to significantly decrease the P activation rate,[23] suggesting that new processes are necessary to remove carbon of the dopant carrying molecules before the high temperature drive-in thermal treatment.

Recently, we synthetized narrow molar mass distribution polymers terminated with P-containing moieties. These dopant-carrying polymers were thermally grafted to the not-deglazed and deglazed silicon substrates from the melt.[24-26] Due to the self-limiting nature of the "grafting-to" reaction, these molecules form a brush layer, whose thickness depends on the molar mass of the employed dopant polymer, irrespective of the oxidation of the Si surface. Efficient tuning of the areal density of the grafted molecules over the target substrate and consequently the final number of P atoms in the dopant source was demonstrated. Polymeric chains were removed by a plasma treatment before the deposition of the SiO_2 capping layer, acting as diffusion barrier during the drive-in process. Subsequent injection and activation of P atoms into the Si substrate, with negligible carbon and oxygen contaminations, was achieved by high temperature annealing.[24] Repeated cycles of grafting and O_2 plasma removal of the polymeric chains were demonstrated to progressively increase the P dose in the dopant source.[24] In this work, we investigate the efficiency of this doping approach as a function of P areal dose and drive-in processing conditions, to assess the potential of this technology as a feasible solution for the development of a gentle doping platform for next generation microelectronics devices.

Experimental

Materials.

A hydroxy-terminated polystyrene (PS) homopolymer was synthesized by ARGET-ATRP copolymerization of styrene. The sample was subsequently reacted with diethylchlorophosphate (DPP). The resulting P-terminated polymer (PS-P) presents a number average molar mass M_n = 2.3 ± 0.3 kg/mol, polydispersity index Đ = 1.05 ± 0.01, and degree of polymerization N = 17 ± 3. More information about synthesis and characterization of the P-terminated polymer is available in previous publications.[24,25] Substrates were prepared from nearly intrinsic (ρ > 5 kΩ cm) floating zone (FZ) single-side polished Si (100) wafers purchased from Siltronix.

Substrate Cleaning.

Wafers were cleaved into 0.9 x 0.9 cm^2 pieces and treated with Piranha solution (H_2SO_4 and H_2O_2 in a 3:1 ratio) at 80 °C for 40 min, followed by rinsing with deionized water for 5 min. Piranha solution was used to clean the sample surface from all organic impurities and to promote grafting by increasing the surface density of hydroxyl groups. Finally, the samples were dried under N_2 flow, and the native SiO_2 layer thickness was measured by ellipsometry.

Sample Preparation.

The P terminated PS homopolymer was dissolved in toluene (9 mg of homopolymer in 1 ml of toluene) by means of ultrasonic bath for 5 min. Then the solution was spin coated (30 s at 3000 rpm) on the cleaned substrates to form a uniform polymer film. In order to check the thickness uniformity among the different samples, the polymer layer thickness of each sample was measured by ellipsometry. The average thickness of the spin-coated polymer films was determined to be 27.2 ± 0.9 nm. The samples were then annealed using a rapid thermal processing (RTP) apparatus for 15 min at 190°C in N_2 atmosphere in order to promote the grafting reaction, following the procedure described elsewhere.[24] Temperature was selected in order to avoid any thermal degradation of the P terminated polymers during the grafting process.[25,27] During this process, the P containing moiety at the polymer chain end reacts with a hydroxyl group at the SiO_2 surface, ultimately forming a uniform brush layer over the native SiO_2 layer. Non-grafted chains were washed out by ultra-sonic bath in toluene for 5 min. Finally,

Journal of Materials Chemistry C Accepted Manuscript

 This journal is © The Royal Society of Chemistry 20xx

Please do not adjust margins

Published on 19 May 2020. Downloaded by Uppsala University on 5/20/2020 3:40:09 PM.

Journal of Materials Chemistry C Accepted Manuscript

View Article Online
DOI: 10.1039/D0TC01856B

samples were dried under N_2 flow. The thickness of the final grafted polymeric layer was measured by ellipsometry. The average thickness of the polymeric films over the entire set of samples was 2.43 ± 0.08 nm, that is about two times the radius of gyration of the polymer, in agreement with previous reports in the literature.[28] Upon grafting, polymeric chains were removed by O_2 plasma ashing (40W for 5 min) leaving only phosphate groups at the silicon surface. The thickness of the residual polymeric layer after O_2 plasma ashing was monitored to confirm complete removal of the PS chains. Phosphorus concentration on the substrate can be increased by repeated cycles of grafting-ashing. Samples with a number of grafting-ashing cycles ranging from 1 to 5 were prepared to obtain dopant sources with different concentration of P impurity atoms. Once completed the grafting-ashing procedure, the samples were capped with a 10-nm thick SiO_2 layer deposited by e-beam evaporation, forming a P δ-layer source embedded in a SiO_2 matrix. P atoms were diffused through the native SiO_2 barrier into the Si substrate by high temperature thermal treatment performed in a RTP system. In more details, samples were annealed in N_2 atmosphere at temperatures ranging from 1000 to 1250 °C for 5s with a ramp temperature of 50 °C/s. Upon removal of SiO_2 capping layers by HF dipping and subsequent washing in deionized H_2O, aluminum metal contacts were deposited by thermal evaporation using a shadow mask. The metal contacts are circular dots with diameter ~ 1.2 mm placed at the sample corners. A picture of a typical sample with the Al metal contacts is reported in the inset of Figure 1a.

Phosphorous quantification.

Time of Flight Secondary Ion Mass Spectrometry (ToF-SIMS) depth profiles were performed using a dual beam IONTOF IV system operating in negative mode. Cs^+ ions (@ 1 keV and 80 nA) and Ga^+ ions (@ 25 keV and 1 pA) were used for sputtering and analysis, respectively. A 16 nm-thick silicon on insulator reference sample was used to measure sputter velocity and calibrate the depth scale. P concentration profiles were obtained by proper calibration of the P signals in the Si matrix by means of an analytical protocol that is described in previous publications.[29,30]

Electrical Characterization.

Sheet resistance and Hall measurements were performed in a Van der Pauw geometry using a close-cycled cryostat, at temperatures ranging from 100 K and 300 K. A constant current (I) is applied through the Keithley 6221 while the Keithley 2182A nanovoltmeter records the corresponding voltages (V). Current/voltages can be injected/measured in a custom mode across the four aluminum metal contacts, thus allowing to record two-point I-V curves. For Hall measurements, a magnetic field up to 0.8 T is applied. The data are recorded with a custom-written Labview-based acquisition software.

Results and discussion

The injection and activation of P impurity atoms were investigated as a function of the temperature T of the drive-in process. P dopant sources were prepared by a single cycle of grafting and O_2 plasma cleaning over a not-deglazed Si substrate using a P terminated polystyrene (PS) sample (M_n = 2.3 ± 0.3 kg/mol, Đ = 1.05 ± 0.01). To explore the effect of the annealing temperature, P injection and activation in the high resistivity (100) Si substrates were performed by RTP treatments at temperatures ranging from 1000°C to 1250°C for 5 s.
Preliminary analysis of the metal contacts was performed by measuring I-V characteristic at room temperature for each pair of contacts of this set of samples. The representative I-V curves obtained from the samples annealed at 1000°C and 1250°C are reported in figure 1a and figure 1b, respectively. Collected data indicate that annealed at T ≤ 1100°C present a non-linear current voltage characteristic indicating a non-Ohmic behavior of the contacts. Conversely, samples annealed at T ≥ 1150°C exhibit a perfect linear behavior indicating that good Ohmic contacts were formed. It is worth to remember that for contacts with high doping concentration, the barrier width becomes very narrow, and the tunneling current becomes dominant. Accordingly, experimental data suggest that different amounts of P atoms have been introduced into the Si substrate depending on the annealing temperature of the drive-in process. In particular, at high annealing temperatures the P concentration at the metal-semiconductor interface is so high that tunneling is possible across the potential barrier between the metal and the semiconductor, resulting in a Ohmic behavior of the I-V characteristics.[1]

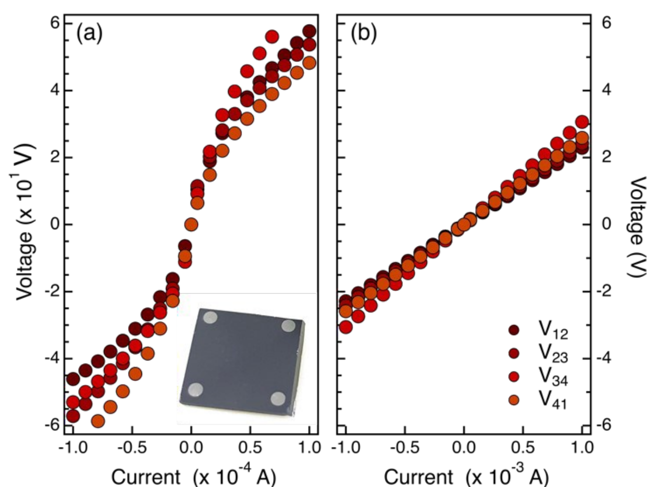

Figure 1: I-V characteristics of the different pairs of contacts for the samples obtained with 1 cycle of grafting-O_2 plasma ashing followed by high temperature annealing in RTP at T = 1000°C (a) and T = 1250°C (b) respectively. For each sample, different I-V curves were acquired, measuring the tension V_{ij} between two adjacent contacts when a current I_{ij} is applied and considering all the possible combinations of adjacent metal contacts i = {1,...,4} and j = i + 1. A picture of a typical 0.9 x 09 cm^2 Si sample with Al metal contacts deposited at each corner is depicted in the inset.

The Sheet resistance (R_s), carrier concentration (σ), and carrier mobility (μ) values for the set of samples annealed in the 1000-1250 °C range are depicted in figure 2. All measurements are recorded in the Van der Pauw geometry through the four aluminum contacts at the corners. In particular, the current (I_{ij})

Please do not adjust margins

View Article Online
DOI: 10.1039/D0TC01856B

Published on 19 May 2020. Downloaded by Uppsala University on 5/20/2020 3:40:09 PM.

is injected between two adjacent *i* and *j = i* +1 contacts, and the voltage drop (V_{kl}) is measured across the opposite *k = i + 2* and *l = k + 1* contacts. A schematic picture of the probe configuration is sketched in the inset of figure 2a. From the measured (I_{ij}, V_{kl}) values, we determined the sheet resistance R_s of the samples. Figure 2a shows the evolution of R_s as a function of the annealing temperature in a 5-s long RTP process for P dopant injection/activation. The black dashed lines indicate the R_s values measured in the high resistivity pristine substrate and in the same sample after annealing at 1250°C for 5 s. The R_s reduction upon high temperature annealing in the high resistivity substrate is associated to the formation of oxygen-related thermal donors.[31,32] The values are reported as a reference to demonstrate the effective modification of the sheet resistance due to the injection and activation of the P impurities into the Si substrate. Collected data indicate a progressive decrease of the sheet resistance R_s as a function of the annealing temperature, in perfect agreement with data reported in our previous work.[24]

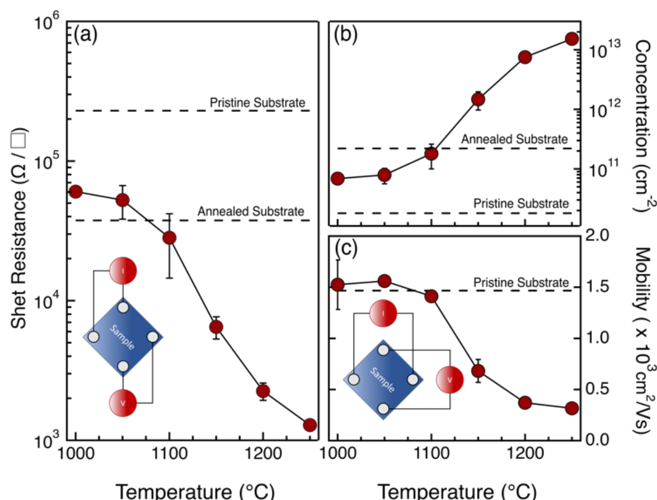

Figure 2: (a) Sheet resistance (R_s) values as function of the annealing temperature (T) during the drive-in process. R_s values of the pristine and annealed (T = 1250°C) substrate are indicated by the black dashed lines. The inset indicates the configuration of the probes on the contacts during van der Pauw measurements. (b) dopant concentration (σ) and (c) carrier mobility (μ) values as function of the annealing temperature (T) during the drive-in process. The corresponding σ and μ values of the pristine substrate are indicated by the black dashed lines. The σ value of the annealed (T = 1250°C) substrate is indicated by the black dashed line. The inset indicates the configuration of the probes on the contacts during Hall effect measurements. Each data point was obtained by repeated measurements performed on two different samples prepared with the same number of grafting-ashing cycles and drive-in treatment.

Hall effects measurements were performed using a van der Pauw configuration with the probes placed at the four corners of the sample, following the arrangement shown in of figure 2c. Current (I_{ik}) was injected between two contacts *i* and *k = i + 2* on the opposite corners of the sample and the voltage drop (V_{jl}) was measured across the other two contacts *j = i* + 1and *l = k + 1*. The carrier concentration σ and the carrier mobility μ were obtained from the analysis of the collected data using a constant doping approximation.[9] Figures 2b and 2c depict the evolution of σ and μ as a function of the annealing temperature T of the drive-in process. The corresponding σ and μ values of

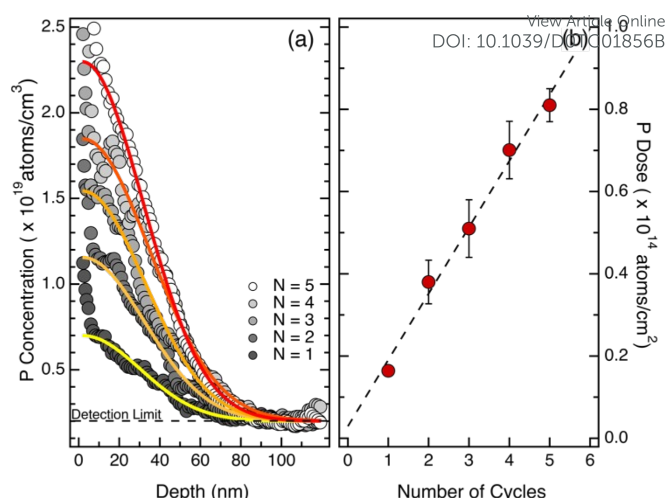

Figure 3: (a) ToF-SIMS calibrated depth profiles showing P distribution in the silicon substrate upon annealing at 1200 °C for 5 s. The P concentration in the dopant source was progressively increased by cycles of grafting-O_2 plasma on a not-deglazed Si (100) substrate using a P terminated PS polymer. Grafting was performed at 190°C in N_2 atmosphere. A 10 nm-thick SiO_2 capping layer was deposited on the sample to prevent P out-diffusion during the drive-in process and subsequently removed prior to ToF-SIMS characterization. P calibrated profiles were fitted (continuous lines) assuming a limited source model. The black dashed line indicates the P detection limit of the ToF-SIMS apparatus. (b) Total P dose as function of the number of grafting- O_2 plasma cycles. Total P doses were determined by integration of the P distribution obtained from the calibrated ToF-SIMS profiles. Each data point was obtained by repeated measurements performed on two different samples prepared with the same number of grafting-ashing cycles and drive-in treatment

the pristine high resistivity substrate are indicated by the black dashed lines. The σ value of the annealed (1250°C, 5 s) substrate is indicated in figure 2b by the black dashed line. The increase of carrier concentration upon annealing in the undoped high resistivity substrate is associated to the formation of thermal donors. The concentration of thermal donors upon annealing is determined to be ~ 2 x 10^{11} cm^{-3}, in perfect agreement with literature data.[32] Increasing the annealing temperature, we observed a progressive increase in the carrier concentration and a concomitant reduction of carrier mobility, in accordance with literature data.[1,9] It is interesting to note that, at annealing temperatures T ≤ 1100°C, the σ values exhibit a limited variation with respect to pristine substrate and the corresponding μ values are perfectly consistent with n-type carrier mobility in intrinsic or low doped silicon.[1] Conversely, at T ≥ 1150 °C, data indicate a significant enhancement of the concentration of mobile charges σ, that corresponds to a substantial drop of the carrier mobility μ. The measured μ values suggest that, in samples annealed at T ≥ 1150 °C, dopant concentrations in the surface layer of the sample is expected to be $\rho \geq 1 \times 10^{18}$ cm^{-3}.[1] These results are perfectly consistent with the observed formation of good Ohmic contacts for samples annealed at T ≥ 1150 °C. The high temperature required to promote effective P diffusion and activation in the Si substrate is essentially associated to the presence of a 1.5 nm thick native SiO_2 film on the surface of the not-deglazed silicon substrate. In fact, P diffusion in SiO_2 is very slow even at relatively high temperatures.[33-36] Accordingly, the

Journal of Materials Chemistry C Accepted Manuscript

 This journal is © The Royal Society of Chemistry 20xx

Please do not adjust margins

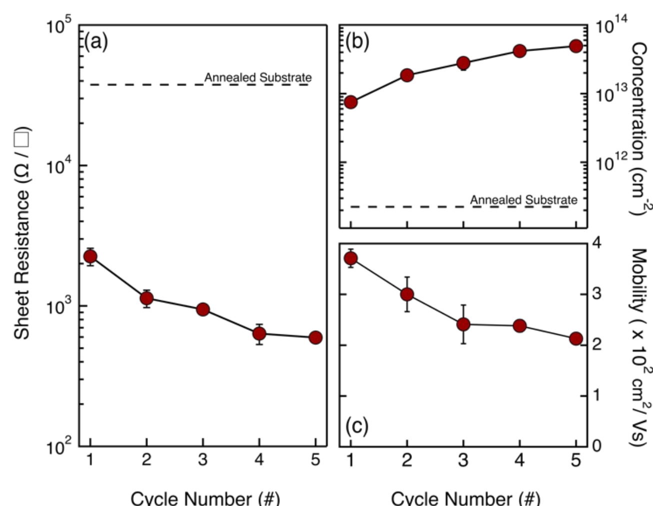

Figure 4: *(a) Sheet resistance R_s, (b) carrier concentration σ and (c) carrier mobility μ as a function of the number of grafting-O_2 plasma cycles. Each data point was obtained by repeated measurements performed on two different samples prepared with the same number of grafting-hashing cycles. R_s and σ values of the annealed substrate are indicated by the black dashed lines.*

native SiO_2 film represents a diffusion barrier that prevents efficient P injection into the Si substrate unless very high temperatures (T ≥ 1100 °C) are applied.[33] In this respect, it is interesting to focus on the high temperature processes, in order to generate high dopant concentration in the region close to the surface layer of the silicon substrate.

To investigate the possibility to effectively modulate the dose of P atoms injected into the Si substrate, a second set of samples was prepared with repeated cycles of grafting and O_2 plasma ashing over a not-deglazed Si substrate using the same P-terminated PS molecules. The number of grafting-ashing cycles was varied from 1 to 5 in order to progressively increase P concentration in the dopant sources. The drive-in process was performed in RTP using the same processing conditions (T = 1200°C, t = 5 s) for all the samples. ToF-SIMS analysis was carried out to characterize the doping profile of the thermally diffused P atoms in silicon. Calibration of the P signals in the Si matrix was performed applying previously developed protocols.[29] Figure 3a shows the calibrated ToF-SIMS depth profiles of P in the Si substrate upon drive-in, for the samples with dopant sources obtained with a different number of grafting-ashing cycles. Due to the presence of a native oxide and to well-known artifacts characterizing the initial stages of SIMS analysis,[37] the effective quantification of P concentration in the depth profile is not reliable in the so-called transient region, i.e. in the region close to the surface of the sample. From a general point of view, all the samples exhibit a high surface concentration that sharply decreases to 10^{18} atoms/cm^3 within the initial 80 nm of the Si substrate. The maximum surface concentration ranges from 0.7 x 10^{19} to 2.5 10^{19} atoms/cm^3, depending on the concentration of P in the dopant source, i.e. on the number of grafting-ashing cycles. It is worth to note that, in principle, P concentration could be further enhanced by increasing the number of grafting/ashing cycles. ToF-SIMS data were fitted using Gaussian curves (continuous lines in figure 3a) neglecting the data points in the initial 5 nm from the sample surface to account for artifacts in the ToF-SIMS depth profile. The Gaussian functions are characterized by a constant standard deviation (σ = 30.3 ± 2.4 nm) consistent with a source limited model for P diffusion in silicon.[1] The total dose of P atoms injected into the silicon substrate was obtained by integration of the calibrated P concentration profiles. Figure 3b reports the P total dose as function of the number of grafting-ashing cycles. A linear increase in the P dose is observed in agreement with the idea that the dose of P atoms in the dopant source grows stepwise with each cycle.

View Article Online
DOI: 10.1039/D0TC01856B

Van der Pauw analysis and Hall effect measurement were performed on these samples to obtain information about electrical activation of the injected P impurity atoms. Figure 4 reports the values of sheet resistance R_s (a), carrier concentration σ (b) and electron mobility μ (c) as a function of the number of grafting-ashing cycles. Data highlight the progressive R_s reduction determined by the increase in σ that is associated to the higher concentration of P impurity atoms introduced into the Si substrate during the drive-in process. Once again, the gradual decrease of electron mobility μ perfectly correlates with the expected carrier mobility reduction in case of high dopant concentrations.[1] Data suggest that the effective concentration of active dopants in the Si substrate can be properly modulated by changing the amount of P atoms in the dopant source.

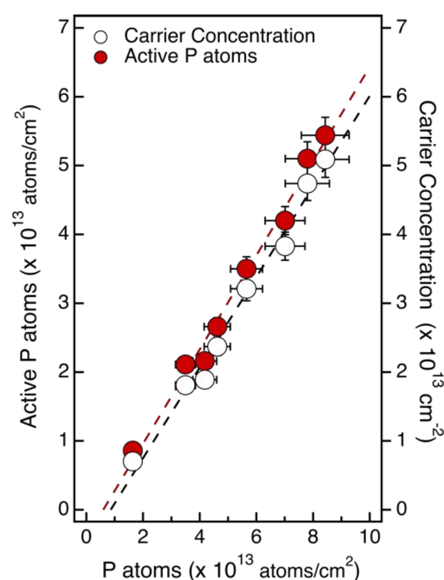

Figure 5: Carrier concentration and concentration of active P impurity atoms as a function of the ToF-SIMS dose of P atoms for the samples obtained by multiple grafting-O_2 plasma cycles. Concentration of active P impurity data was obtained from Hall effect measurements using a uniform layer approximation. The linear fits of the experimental data are indicated by dashed lines.

Figure 5 reports the free electron concentrations obtained by room temperature Hall effect measurements in uniform layer approximation versus the ToF-SIMS dose of P atoms for the samples obtained by multiple grafting-ashing cycles. Data exhibit a good linear trend, further confirming that electrical properties of the Si substrate can be finely tuned by varying the phosphorus concentration in the dopant source. From the slope

Published on 19 May 2020. Downloaded by Uppsala University on 5/20/2020 3:40:09 PM.

Journal of Materials Chemistry C Accepted Manuscript

Please do not adjust margins

View Article Online
DOI: 10.1039/D0TC01856B

Published on 19 May 2020. Downloaded by Uppsala University on 5/20/2020 3:40:09 PM.

Journal of Materials Chemistry C Accepted Manuscript

of the linear fit we obtain the ratio between the free electrons and the phosphorus atoms that corresponds to 66.7%. Gao *et al.* reported a ratio between the free electron and the phosphorus atoms of 66.6% in a silicon sample doped by MLD, using P containing low molar mass molecules that are quite different from those employed in the present work.[23] Conversely Wu *et al*. obtained a value of 26.7% using another P containing molecule.[38] This low ratio was explained by observing that electrons ionized from the P dopants were mostly trapped by deep level defects, that are likely carbon interstitials.[23]

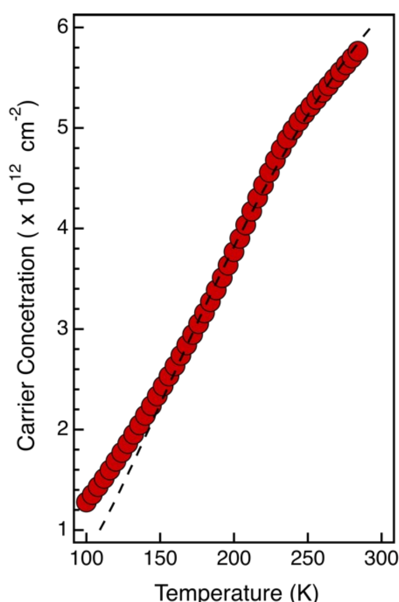

Figure 6: Carrier concentration versus temperature obtained from Hall measurements at different T of a sample prepared with a single grafting/ashing cycle. Drive-in of the dopants was performed by annealing the smaple in RTP at T = 1200°c for 5 s. Red dashed line corresponds to the fitting of the data using the standard model reported in ref. 23.

To obtain information about the activation efficiency of the doping process, it is necessary to determine the ionization rate of the P atoms incorporated into the Si substrate. When P concentrations is higher than 1 x 10^{17} cm^{-3}, only a fraction of the substitutional P impurity atoms incorporated into the Si crystal lattice is ionized, even at room temperature. Using the theoretical model of incomplete ionization proposed by Altermatt et al.,[39] the ionization rate (η_i) was calculated for the different samples. Considering the free electron concentration determined by analysis of Hall measurements in constant doping approximation and the ionization rate η_i of the different samples, we determined the fraction of active P atoms in each sample. Figure 5 reports the values of the active fraction of P atoms as a function of the ToF-SIMS dose of P atoms for the samples obtained by multiple grafting-ashing cycles. The linear fit of the experimental data provides an activation efficiency η_a = 69.3 ± 3.2 %.

To countercheck the nature and concentration of the active dopant impurities, low temperature Hall measurements were performed on the sample obtained with a single grafting/ashing cycle and annealed at 1200°C for 5 s. Acquisition temperatures were varied from 300 K to 100 K. Data acquired at different temperature were analyzed using a constant doping approximation to determine the carrier concentration. Figure 6 reports the electron concentration as a function of acquisition temperature. By fitting these data using the standard model reported by Gao *et al.*[23], we obtained the activation energy (E_a) and the concentration of active P impurity dopants (N_A). In particular, the activation energy is compatible with the value E_a = 45 meV reported in the literature for phosphorus ionization in silicon.[1] The concentration of electrically active P impurity dopants obtained from this analysis is N_A= 9.4 x 10^{12} cm^{-2}, corresponding to an ionization rate η_i = 85%. This value is perfectly consistent, within the experimental error, with the value η_i = 82% calculated for this sample, according to the theoretical model of incomplete ionization proposed by Altermatt et al.[39]

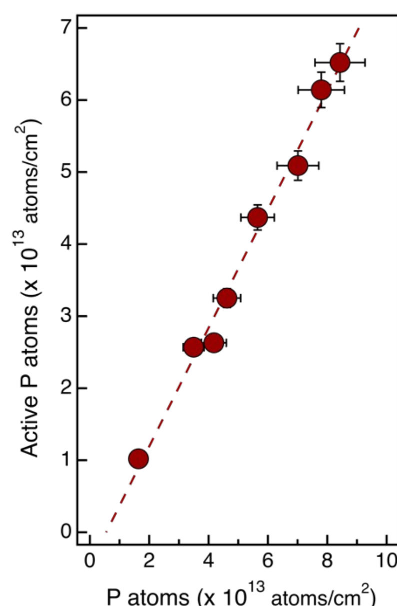

Figure 7: Concentration of active P impurity atoms as a function of the ToF-SIMS dose of P atoms for the samples obtained by multiple grafting-ashing cycles. Concentration of active P impurity atoms was obtained from Hall effect measurements using a multilayer model. Linear fit of the data (red dashed line) indicates an activation efficiency η_a = 83.1 ± 3.6 %.

It is important to note that carrier concentration values obtained from Hall effect measurements using the uniform layer approximation are usually underestimated.[26] Considering the high gradient of P concentration that is observed in ToF-SIMS depth profiles, a more accurate estimation of the effective carrier concentration requires to determine the Hall coefficient R_H using a multilayer model that takes into account the variation of the dopant impurities and the associated variation of carrier mobility.[9,23] On the basis of the ToF-SIMS depth profiles and assuming a Gaussian distribution of P impurity atoms, it is possible to correctly model the electron distribution in the Si substrate and calculate the effective carrier concentration in the samples. Following the same reasoning that was applied in the case of the uniform concentration approximation, the concentration of the active P impurity atoms was determined for the different samples. Figure 7 reports the values of the active fraction of P atoms obtained using the multilayer model

This journal is © The Royal Society of Chemistry 20xx

Please do not adjust margins

View Article Online
DOI: 10.1039/D0TC01856B

as a function of the ToF-SIMS dose of P atoms for the different samples. The linear fit of the experimental data provides an activation efficiency η_a = 83.1 ± 3.6 %.

Discussion.

The main concern about doping strategies using self-assembling molecules is the presence of carbon and oxygen contamination and consequent dopant deactivation. B activation has been demonstrated to be almost full with no impact of carbon impurities.[40] Conversely, recent results demonstrate that the presence of carbon contamination determines the formation of carbon-phosphorus pairs and the consequent deactivation of the P impurity atoms.[23,38,40,41] In a previous experiment using MLD we demonstrated by means of combined ToF-SIMS and atom probe tomography (APT) analysis that carbon contamination is concentrated in a 2-nm thick layer close to the Si surface.[42] A possible solution to overcome the problem of P deactivation determined by C contamination could be the removal of this contaminated layer by calibrated etching protocols. It is interesting to note that, in the case of MLD, high dose P junctions are characterized by relatively high activation efficiency.[23] Conversely, carbon deactivation effect is particularly evident in the case of low dose P junctions. Activation efficiency as low as 7% has been reported for P junctions using super-branched poly-glycerol molecules.[41] This effect can be tentatively attributed to the use of large molecules and consequently to the high level of carbon contamination that is introduced into the Si substrate during the annealing process for dopant drive-in. This fact suggests a limitation for MLD in term of the effective capability to control P dose by changing the steric hindrance of the dopant containing molecules. Formation of the P dopant source on a native SiO_2 layer can reduce the carbon contamination since carbon atoms are trapped at the SiO_2/Si interface, reducing carbon diffusion in the doped substrate when carbon containing precursors are used. Nevertheless, the use of an oxide layer introduces severe limitation in the P drive-in process since high temperatures are necessary to overcome the SiO_2 diffusion barrier, limiting the capability to control the junction depth.

Alternatively, to reduce carbon injection into the substrate, it is necessary to remove the carbon containing molecule before drive-in of the P impurity atoms into the Si substrate. In a previous paper, we demonstrated that O_2 and/or Ar plasma is extremely effective in removing the carbon component of the brush layer formed using homopolymers terminated with P-containing moieties.[24] Accordingly, the level of carbon contamination in the dopant source is much lower than the one obtained using MLD with the same dopant containing moiety that is tethered to one end of the homopolymer chain.[24] It is worth to note that carbon content was determined to be of the order of adventitious carbon that is deposited over the sample substrate during exposure to air before deposition of the SiO_2 capping layer. Moreover, carbon content is independent on the P dose in the source i.e. of the molecular weight of the P terminated polymers or of the number of grafting-ashing cycles. Accordingly, in the present work, the dopant activation was found to be independent on P dose in the range of dopant concentrations that were explored, indicating that no significant P deactivation effects are induced by carbon contamination.

From a more general perspective it is important to compare these data with those reported in the literature in case of high concentration of P impurity atoms into the Si substrate by ion implantation. Activation has been a serious problem for the ion implantation technology. Post-annealing above 800 °C is commonly used for dopant activation[43] and several thermal treatment schemes have been proposed to increase activation efficiency.[44,45] Single step annealing at high temperature yields P activation of the order of 40% - 60%. Conversely, specific thermal treatments decoupling the damage recovery process and crystal regrowth from the electrical activation were demonstrated to significantly improve dopant activation. In 100 keV and 50 keV P implants, 100% and 75% activation of the implanted P atoms are reported, respectively, due to the different depth distribution of implantation damage into the Si substrate.[44] In the case of high fluence low energy ion implantation, significant out diffusion of P impurity atoms is observed during annealing. This out diffusion process is associated to trapping of P at the SiO_2/Si interface with consequent deactivation of the dopant impurities.[46,47] The activation efficiency of P dopants close to the silicon surface is about 55-59%, due to interaction with surface states and hydrogenation phenomena.[47] Accordingly, the ~ 80% activation efficiency in P junctions formed using the proposed self-assembly doping strategies are sufficiently high to compete with current ion implantation technology. In this respect, we believe that the proposed technology represents a valuable alternative to ion implantation for all those applications requesting a simple and low cost approach to precisely control doping of silicon or other semiconductor materials. These layers of tethered P-terminated polymers represent a straightforward solution for the doping of nanostructured materials which cannot be processed using standard ion implantation due to shadowing phenomena, unless expensive and complex protocols are applied. Accordingly, we could envision the application of this technology for the doping of nanostructures substrates for photovoltaic applications, requiring effective approaches to reduce cost of the devices.[48]

Finally, integration of self-assembled doping strategies with conventional lithographic protocols could provide the possibility to generate highly-doped localized regions in Si overcoming the P concentration inducing the metal-semiconductor transition. Few experiments have been reported in literature showing the possibility to localize grafting of dopant containing molecules in a small area with lateral dimension of few nanometers. Those data indicate that self-assembling doping strategies could in principle pave the way to mass fabrication of quantum dots, nanowires and sheets into the Si crystal. In turns, these elements could be used as building blocks for the fabrication of novel devices for quantum computation. Integration of P terminated polymers with advanced lithographic approaches is currently ongoing.

Published on 19 May 2020. Downloaded by Uppsala University on 5/20/2020 3:40:09 PM.

Journal of Materials Chemistry C Accepted Manuscript

Please do not adjust margins

Published on 19 May 2020. Downloaded by Uppsala University on 5/20/2020 3:40:09 PM.

View Article Online
DOI: 10.1039/D0TC01856B

Journal of Materials Chemistry C Accepted Manuscript

Conclusions

Polystyrene polymers with narrow molar mass distribution and end-terminated with a P containing moiety were grafted to a not-deglazed high resistivity Si substrate to build up a phosphorus δ-layer embedded in a SiO_2 matrix. Subsequent drive-in of P-atoms into the Si substrate was obtained by high temperature (1000-1250°C) thermal treatments in RTP. Temperature-dependent resistivity and Hall measurements in the Van der Paw configuration were performed to investigate injection and activation of the P atoms into the Si substrate. High activation rates (η_a > 80%) of injected P atoms were achieved in the specific range of P concentrations explored in this work. According to these data, this bottom-up approach provides an effective doping technology that guarantees accurate control of the number of P atoms that are injected during the drive-in process into a semiconductor substrate. The high activation of the P atoms suggests this process could represent a valuable alternative to conventional ion implantation in samples that can no withstand implantation induced crystal damages. Further experiments are currently investigating the integration of this doping approach with conventional lithography in order to control lateral distribution of dopant containing molecules over the substrate at nanoscale.

Conflicts of interest

"There are no conflicts to declare".

Acknowledgements

The authors would like to thank Mario Alia (IMM-CNR) and Simone Cocco (IMM-CNR) for their help with clean room processes and electrical characterization of the samples, respectively.

Notes and references

1 S. M. Sze and K. K. Ng, *Physics of Semiconductor Devices*, John Wiley & Sons, Inc., 2007.
2 N. Sano and M. Tomizawa, *Appl. Phys. Lett.*, 2001, **79**, 2267.
3 T. Shinada, S. Okamoto, T. Kobayashi, and I. Ohdomari, *Nature*, 2005, **437**, 1128–1131.
4 P. A. Stolk, H.-J. Gossmann, D. J. Eaglesham, D. C. Jacobson, C. S. Rafferty, G. H. Gilmer, M. Jara´ız, and J. M. Poate, H. S. Luftman, T. E. Haynes, *J. Appl. Phys.*, 1997, **81** (9), 6031-6050.
5 J. O'Connell, G. A. Verni, A. Gangnaik, M. Shayesteh, B. Long, Y. M. Georgiev, N. Petkov, G. P. McGlacken, M. A. Morris, R. Duffy, and J. D. Holmes, *ACS Appl. Mater. Interfaces*, 2015, **7**, 15514–15521.
6 C. Qin, H. Yin, G. Wang, Y. Zhang, J. Liu, Q. Zhang, H. Zhu, C. Zhao, H.H. Radamson *J. Mater Sci: Mater in Electronics*, 2020, **31**, 98–104
7 P. K. Chu, S. Qin, C. Chan, N. W. Cheung, and L. A. Larson, *Mater. Sci. Eng. R Reports*, 1996, **17**, 207–280.
8 M. L. Hoarfrost, K. Takei, V. Ho, A. Heitsch, P. Trefonas, A. Javey, and R. A. Segalman, *J. Phys. Chem. Lett.*, 2013, **4**, 3741–3746.
9 J. C. Ho, R. Yerushalmi, Z. Jacobson, Z. Fan, R. L. Alley, and A. Javey, *Nat. Mater.*, 2008, **7**, 62–67.
10 R. C. Longo, K. Cho, W. G. Schmidt, Y. J. Chabal, P. Thissen, *Adv. Funct. Mater.*, 2013, **23**, 3471–3477.
11 K.W. Ang, J. Barnett, W.Y. Loh, J. Huang, B. G. Min, P. Y. Hung, I. Ok, J. H. Yum, G. Bersuker, M. Rodgers, V. Kaushik, S. Gausepohl, C. Hobbs, P. D. Kirsch, R. Jammy, *Technol. Dig. - Int. Electron Devices Meet.*, IEDM 2011, 35.5.1–35.5.4.
12 J. C. Ho, A. C. Ford, Y. L. Chueh, P. W. Leu, O. Ergen, K. Takei, G. Smith, P. Majhi, J. Bennett, A. Javey, *Phys. Lett.*, 2009, **95**, 72108.
13 J. H. Yum, H. S. Shin, R. Hill, J. Oh, H.D. Lee, R. M. Mushinski, T. W. Hudnall, C. W. Bielawski, S. K. Banerjee, W. Y. Loh, W.-E.; Wang, P. A. Kirsch, *Appl. Phys. Lett*., 2012, **101**, 253514.
14 K. R. Kort, P. Y. Hung, P. D. Lysaght, W. Y.; Loh, G. Bersuker, S.; Banerjee, *Phys. Chem. Chem. Phys.*, 2014, **16**, 6539–6543.
15 E. Y. J. Kong, P. Guo, X. Gong, B. Liu, Y. C. Yeo, *IEEE Trans. Electron Devices*, 2014, **61**, 1039–1046.
16 K. Cho, D. J. Ruebusch, M. H. Lee, J. H. Moon, A. C. Ford, R. Kapadia, K. Takei, O. Ergen, A. Javey, *Appl. Phys. Lett*., 2011, **98**, 203101.
17 B. Long, B.; G. A. Verni, J. O'Connell, J. Holmes, M. Shayesteh, D. O'Connell, R. Duffy, Ion. Implant. Technol., Int. Conf. Ion Impl. Technol. 20th 2014, 1–4.
18 F. Sgarbossa, G. Maggioni, G. Andrea Rizzi, S. M. Carturan, E. Napolitani, W. Raniero, C. Carraro, F. Bondino, I. Píš, D. De Salvador, *Applied Surface Science*, 2019, **496**, 143713.
19 F. Sgarbossa, S. M. Carturan, D. De Salvador, G. A. Rizzi, E. Napolitani, G. Maggioni, W. Raniero, D. R. Napoli, G. Granozzi, A. Carnera, *Nanotechnology*, 2018, **29** (46), 465702.
20 N. Kennedy, R. Duffy, G. Mirabelli, L. Eaton, N. Petkov, J. D. Holmes, B. Long, C. Hatem, L. Walsh, *J. Appl. Phys.*, 2019, **126**, 025103.
21 L. Ye, S. P. Pujari, H. Zuilhof, T. Kudernac, M. P. de Jong, W. G. van der Wiel, J. Huskens, *ACS Appl. Mater. Interfaces*, 2015, **7**, 3231–3236.
22 M. L. Hoarfrost, K. Takei, V. Ho, A. Heitsch, P. Trefonas, A. Javey, R. A. Segalman, *J. Phys. Chem. Lett.*, 2013, **4**, 3741–3746.
23 X. Gao, B. Guan, A. Mesli, K. Chen, Y. Dan, *Nat. Comm*., 2018, **9**, 118.
24 M. Perego, G. Seguini, E. Arduca, A. Nomellini, K. Sparnacci, D. Antonioli, V. Gianotti, M. Laus, *ACS Nano*, 2018, **12**, 178–186.
25 V. Gianotti, D. Antonioli, K. Sparnacci, M. Laus, C. Cassino, F. Marsano, G. Seguini, M. Perego, *J. Anal. Appl. Pyrolysis*, 2017, **128**, 238–245.
26 R. Chiarcos, V. Gianotti, M. Cossi, A. Zoccante, D. Antonioli, K. Sparnacci, M. Laus, F. E. Caligiore, M. Perego, *ACS Appl. Electron. Mater.*, 2019, **1** (9), 1807-1816.
27 V. Gianotti, D. Antonioli, K. Sparnacci, M. Laus, T. J. Giammaria, F. Ferrarese Lupi, G. Seguini, M. Perego, *Macromolecules*, 2013, **46** (20), 8224-8234.
28 K. Sparnacci, D. Antonioli, V. Gianotti, M. Laus, F. Ferrarese Lupi, T. J. Giammaria, G. Seguini, M. Perego, *ACS Appl. Mater. Interfaces* 2015, **7**, 10944–10951.
29 M. Mastromatteo, E. Arduca, E. Napolitani, G. Nicotra, D. De Salvador, L. Bacci, J. Frascaroli, G. Seguini, M. Scuderi, G. Impellizzeri, C. Spinella, M. Perego, A. Carnera, *Surf. Interface Anal.*, 2014, **46**, 393–396.
30 M. Perego, G. Seguini, A. Arduca, J. Frascaroli, D. De Salvador, M. Mastromatteo, A. Carnera, G. Nicotra, M. Scuderi, C. Spinella, G. Impellizzeri, C. Lenardi, E. Napolitani, *Nanoscale,* 2015, **7**, 14469–14475.
31 T. Gregorkiewicz, H. H. P. Th. Bekman, *Materials Science and Engineering B,* 1989, **4**, 291-297.
32 L. Capello, I. Bertrand, O. Kononchuk, *Phys. Status Solidi A*, 2017, **214** (7), 1700275.
33 M. Mastromatteo, D. De Salvador, E. Napolitani, E. Arduca, G. Seguini, J. Frascaroli, M. Perego, G. Nicotra, C. Spinella, C.

This journal is © The Royal Society of Chemistry 20xx

Please do not adjust margins

View Article Online
DOI: 10.1039/D0TC01856B

Lenardi, A. Carnera, *J. Mater. Chem. C*, 2016, **4**, 3531-3539.
34 M. Kuisl, E. Sasse, *Thin Solid Films*, 1980, **65**, 373.
35 C. T. Sah, H. Sello, D. A. Tremere, *J. Phys. Chem. Solids*, 1959, **11**(3), 288–298.
36 K. Shimakura, T. Suzuki, Y. Yadoiwa, *Solid-State Electronics*, 1975, **18**(11), 991.
37 A. Benninghoven, F. G. Ruedenauer, H. W. Werner, *Secondary Ion Mass Spectrometry-Basic Concepts, Instrumental Aspects, Applications and Trends*, Wiley, New York, 1987, Vol. 86.
38 H. Wu, K Li, X. Gao, Y. Dan, *AIP Advances*, 2017, **7**, 105310.
39 P. P. Altermatt, A. Schenk, G. Heiser, *J. Appl. Phys.*, 2006, **100**, 113714.
40 J. Fu, K. Chen, S. Chang, K. Zhi, X. Gao, H. Wei, Y. Dan, *AIP Advances*, 2019, **9**, 125219.
41 H. Wu, B. Guan, Y. Sun, Y. Zhu, Y. Dan, *Scientific Reports*, 2017, **7**, 41299.
42 Y. Shimizu, H. Takamizawa, K. Inoue, F. Yano, Y. Nagai, L. Lamagna, G. Mazzeo, M. Perego, E. Prati. *Nanoscale*, 2014, **6**,706–710.
43 A. Shima, A. Hiraiwa, *Jpn. J. Appl. Phys.*, 2006, **45**, 5708.
44 N. Yu, K. B. Ma, C. Kirschbaum, K. Varahramyan, W. K. Chu *Appl. Phys. Lett.*, 1993, **63**, 1125-1127.
45 T. Sameshima, K. Yasuta, M. Hasumi, T. Nagao, Y. Inouchi, *Appl. Phys. A*, 2018, **124**, 228
46 X. Zhang, D. Connelly, H. Takeuchi, M. Hytha, R. J. Mears, L. M. Rubin, T.-J. K. Liu, *J. Vac. Sci. Technol. B*, 2018, **36**(6), 061211.
47 S. J. Park, N. Uchida, H. Arimoto, T. Tada, *Jpn. J. Appl. Phys.*, 2015, **54**, 111302.
48 R.A. Puglisi, C. Garozzo, C. Bongiorno, S. Di Franco, M. Italia, G. Mannino, S. Scalese, A. La Magna, *Solar Energy Materials & Solar Cells*, 2015, **132**, 118–122.

Published on 19 May 2020. Downloaded by Uppsala University on 5/20/2020 3:40:09 PM.

Journal of Materials Chemistry C Accepted Manuscript

This journal is © The Royal Society of Chemistry 20xx

Please do not adjust margins

View Article Online
DOI: 10.1039/D0TC01856B
Published on 19 May 2020. Downloaded by Uppsala University on 5/20/2020 3:40:09 PM.
Journal of Materials Chemistry C Accepted Manuscript